Characterization of DBD plasma actuators located on a rounded trailing-edge aerofoil

S. Baleriola, A. Leroy, S. Loyer, P. Devinant, S. Aubrun
Université d'Orléans, INSA-CVL, PRISME, EA 4229, F-45072, Orléans, France

Abstract— This paper presents the characterization of the plasma actuators used to implement a circulation control over a wind turbine airfoil with a rounded trailing edge in order to reduce the aerodynamic load fluctuations on blades. Three sets of multi DBD plasma actuators with different positioning around the trailing edge are studied. These actuators create a tangential jet along the curved model wall. The topology and the strength of the wall jet are investigated by using particle image velocimetry (PIV).

Keywords— DBD plasma actuators, active circulation flow control, wind turbine blade

I. INTRODUCTION

Wind energy is one of the most promising renewable energies for the years to come but there is room for further improvement in wind turbine technology. For instance, wind turbines operate in the atmospheric boundary layer which is highly inhomogeneous and unsteady and induces important load fluctuations on the blades that can reduce their operating durability.

A solution to alleviate these fluctuations is the implementation of an active circulation flow control via plasma actuators in the vicinity of the rounded trailing-edge of an aerofoil. This actuation modifies the orientation of the flow at the trailing edge in order to regulate the lift force via a circulation control, with the ultimate target of maintaining a constant blade load whatever the incoming flow conditions (wind speed and/or angle of attack).

A large number of experimental and numerical studies investigated circulation control on aerofoils ([1], [2]). Most of them deal with fluidic tangential jets that permit a circulation control and the use of the Coanda effect over a curved surface allowing the flow to adhere the curved wall. One common application is the actuation at the trailing edge of an airplane wing in order to replace the mechanical moving parts such as control surfaces or flaps. Nowadays, the circulation control technique is investigated with wind turbine applications in view [3].

Dielectric Barrier Discharge (DBD) plasma actuators are interesting devices regarding their ability to modify the flows in a completely electrical way. One can find in [4] a review of the electrical and mechanical characteristics of DBD plasma actuators applied to airflow control. In order to take advantages of the Coanda effects along curved surface, it is usually necessary for conventional fluidic jets to be characterized by a high momentum coefficient as exposed in [1]. Although the flow mass rate of the induced tangential jet by DBD actuators remains low compared to fluidic jets, the induced jet is supposed to adhere to curved surfaces because the ionic wind is generated by momentum transfer occurring very close to the electrodes following the electric field distribution.

A few studies focus on circulation flow control around wind turbine blades using plasma actuators. Numerical [5] and experimental studies ([6], [7]) show promising results of this control strategy implementation.

In this work multi-DBD and elongated-DBD [8] plasma actuators are used to manipulate the flow around a modified NACA65_4-421 aerofoil, which is circulation control oriented by means of a rounded trailing edge (see Figure 1). The model chord is 300mm, wingspan is 1.1m, and the curvature radius of the trailing edge is 2% of the chord (6mm).

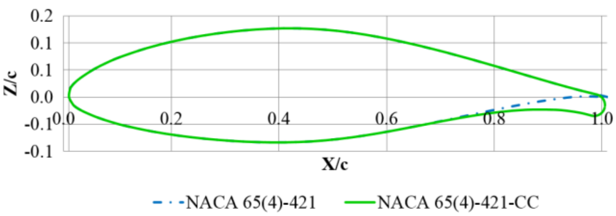

Figure 1 - Original NACA65_4-421 airfoil (dotted line) and circulation control airfoil (solid line)

In order to understand as well as possible the plasma actuation effects on the surrounding fluid and its vicinity, this first study focuses on the characterization of the wall curved jet in quiescent air conditions, before testing it on the aerofoil with an incoming flow. Flow measurement is performed via Particle Image Velocimetry (PIV) and the topology of the plasma jet along the curved surface is characterized for three sets of actuators. The most relevant results of this characterization are presented in the following.

Corresponding author: Sophie Baleriola
e-mail address: sophie.baleriola@univ-orleans.fr

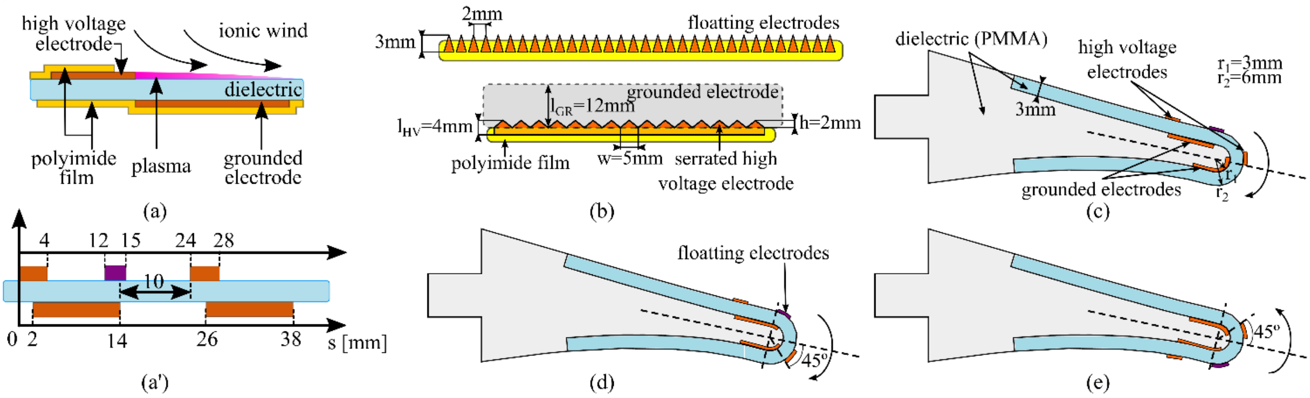

Figure 2 - (a) Working principle of a plasma actuator, (a') Electrode positioning as a function of the curvilinear abscissa *s* represented in a plane configuration (b) top view of the electrodes' geometry, (c) positioning of the electrodes for the actuator 1 (ACT1 multi-DBD, downward effect), (d) ACT2 elongated-DBD, downward effect, (e) ACT3 multi-DBD, upward effect

II. METHODOLOGY

A. *Design of the plasma actuators*

A scheme of the working principle of a DBD (Dielectric Barrier Discharge) plasma actuator can be found in figure 2-a. With a high voltage application at the active electrode (high voltage electrode), the ambient air is ionized and accelerated, creating an ionic wind along the grounded electrode that permits the manipulation of the flow near the wall zone.

The DBD plasma actuators studied in this project consist in two pairs of copper electrodes (45µm-thick) separated by a 3mm thick dielectric material (PMMA). All the actuators are characterized with and without floating electrodes [8]. These electrodes are neither grounded nor connected to the high voltage power supply and allow the expansion of the plasma as well as the homogenization of the plasma along the wingspan. The term *multi-DBD* will be used for the configurations *without* floating electrodes; on the other hand, the configurations *with* floating electrodes will be named as *elongated-DBD*. The positioning of the electrodes developed on a flat surface is shown in figure 2-a' and the electrodes' geometry is shown in figure 2-b. The high voltage electrodes are 4mm wide, serrated and powered by an AC-power supply up to 20kV while the grounded ones are 12mm wide, linear and are encapsulated with the dielectric material of the model itself. The floating electrodes consist in 3mm wide separated copper tooth. The high voltage and the floating electrodes are partially insulated (only tips of the saw teeth are exposed to ambient air). There is a 2mm overlap between the grounded and the active electrodes. The two couples of actuators are spaced out by 10mm and the floating electrodes are 1mm shifted with respect to the first grounded electrode edge. The spanwise length of all the actuators is between 850mm and 950mm.

Figures 2-c, 2-d and 2-e show the arrangement of the electrodes around the trailing edge of the airfoil. Depending on the electrode positioning, the plasma actuator will enable a lift increase (2-c and 2-d) or a lift decrease (2-e).

B. *Power consumption*

The actuator is powered by a laboratory-made power supply and is tested with sinusoidal signals of variable amplitude and frequency (V = 10kV-20kV, f = 500Hz-1500Hz) in a continuous actuation mode. The power consumption of the characterized plasma actuators is measured with the Manley's method. A capacitor (C=47nF, charge ±Q) is placed between the grounded electrode and the earth of the electrical system while the plasma voltage is measured with a high voltage probe.
The energy P dissipated by the discharge during one cycle is given by the following formula:

$$P = f \int_{cycle} V(t)dQ$$

where V(t) is the voltage, Q the capacitor charge and f the frequency of the sinusoidal signal.

Figure 3 shows the electrical power consumption as a function of the applied voltage for the actuator ACT2 in a multi-DBD configuration (without floating electrodes). One can see on figure 4 the power consumption for the same actuator as a function of the applied frequency.

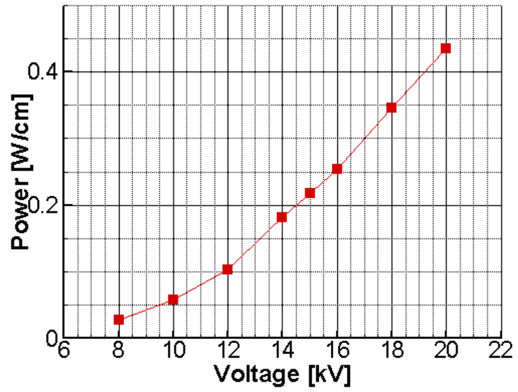

Figure 3 - Electrical power consumption as a function of the applied voltage (f=1kHz) for ACT2 in multi-DBD configuration

The trends obtained are consistent with the ones expected and described in Forte et al. [9]: power consumption increases according to a square law with voltage as mentioned for thick dielectrics [10] and linearly with the frequency.

The power consumption is very similar for the three tested actuator configurations described above. Furthermore, the elongated-DBD configurations give no significant difference in power consumption compared with the multi-DBD ones.

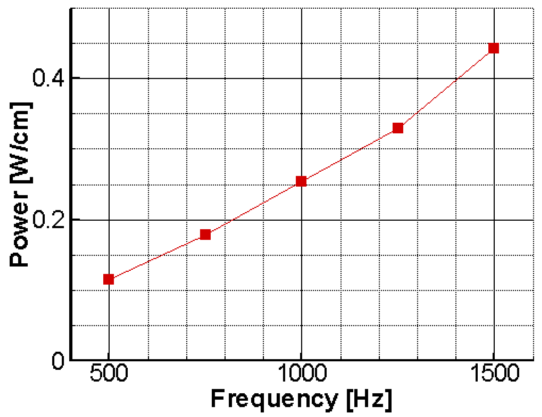

Figure 4 - Electrical power consumption as a function of the applied frequency (V=16kV) for ACT2 in multi-DBD configuration

III. CHARACTERIZATION OF THE INDUCED FLOW IN QUIESCENT AIR CONDITIONS

Mean velocity fields around the trailing edge are obtained with PIV (Particle Image Velocimetry) measurements in the median plane of the airfoil model. The PIV system consists in a Nd:Yag laser (λ = 532 nm, 2x200mJ) emitting pulses with a 4Hz emission rate. Seeding particles are micro-sized olive oil droplets sprayed by a PIVTEC seeding system. Images are acquired with a TSI Power View camera (2048px x 2048px) and a 200mm lens. Data acquisition and processing were performed using the TSI PIV Insight 4GTM data acquisition and analysis software. The investigated flow field is centered on the trailing edge and is 60mm x 60mm. Two consecutive images are recorded with a time interval equal to 58µs, scaling to the maximal velocity of the plasma jet. The final resolution is one vector every 0.5mm with a 32px x 32px interrogation window. Six hundred image pairs are recorded for every configuration. The data in the areas close to the model wall are not available due to laser sheet reflections and plasma light emission. The first velocity vectors considered as relevant are 1mm and above from the model surface.

A. Influence of the electrode position over the trailing edge

The influence of the electrodes' position over the trailing edge is analyzed comparing the effects of actuators ACT1 and ACT2, both meant to increase the lift. As shown on figures 2-c and 2-d, their geometry is identical, but their position along the trailing edge is different: while actuator ACT1 is centered on the edge curvature, actuator ACT2 is shifted towards the underside of the airfoil with an angle of 45º.

This positioning has an effect on the plasma jet created by the actuation. Figures 5 and 6 show the time averaged magnitude velocity field of the flow induced by the actuators ACT1 and ACT2 respectively. Some velocity profiles are superimposed at different curvilinear abscissas. They are obtained by interpolating the PIV measurement points along the corresponding normal lines to the model surface. The position of the electrodes along the dielectric is also shown on the figures.

For the two actuators, as it is observed for ionic wind induced along a flat surface, the three particular zones can be identified in the flow field: one suction area, where the ambient air is carried along towards the electrodes; one acceleration zone located upon the copper electrodes where the air is accelerated and the ionic wind reaches its maximum velocity (around 4m/s) and finally, one area where the plasma diffuses along the wall model. The induced wall jet is supposed to remain attached along the curved surfaces because the ionic wind is generated by momentum transfer occurring very close to the electrodes.

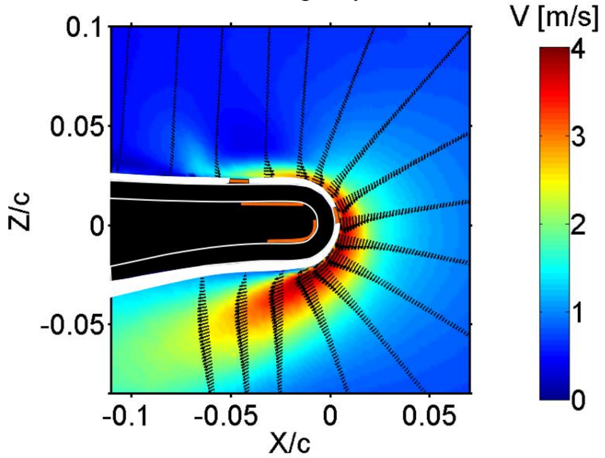

Figure 5 - Time averaged magnitude velocity contours and velocity vector profiles of the flow induced by the actuator 1 (ACT, multi-DBD) in quiescent air conditions (V=18kV, f=1kHz)

However, the topology of the induced flow is very different for the two actuators. For the one centered on the trailing edge, the produced fluid jet follows the model curvature but separates from the wall after the 180º turn: it diffuses and gets thicker, as it can be observed for wall jet flowing around a circular cylinder presented in [11]. With actuator ACT2, the fluid jet follows the model wall curvature, even after the sharp turn, but is thinner than the one with actuator ACT1 and the highest flow velocity area is closer to the wall.

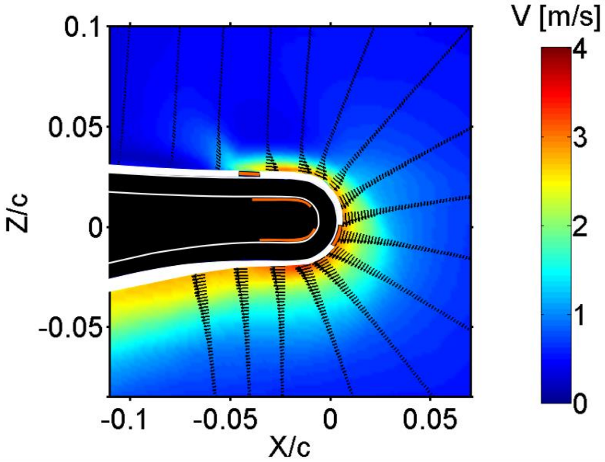

Figure 6 - Time averaged magnitude velocity contours and velocity vector profiles of the flow induced by the actuator 2 (ACT2, multi-DBD) in quiescent air conditions (V=18kV, f=1kHz)

B. Analysis of a non-attached flow configuration

The fluid jet does not always remain attached to the wall depending on the position of the electrodes and the high voltage amplitude. The actuator ACT3 in the multi-DBD configuration, meant for lift decrease, has an unsteady behavior when working with a voltage higher than 16kV. The flow produced by the first DBD does not always follow the rounded trailing edge whereas the flow produced by the second DBD is attached to the upper airfoil surface. Therefore, the whole flow topology alternates between two different states: one where both jets are attached to the wall, and another one, where the first jet separates from the wall and the second one adheres the model surface.

Figure 7 shows the position and the size of the window that is chosen to sort the instantaneous velocity fields in order to highlight these two states. The spatially averaged velocity inside the window as a function of the PIV image number for three independent PIV sets is plotted in figure 8.

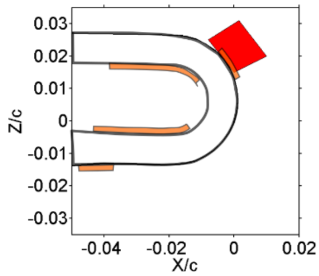

Figure 7 - Position and size of the spatially averaged window

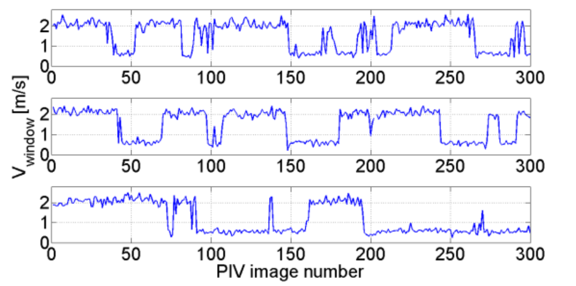

Figure 8 - Window spatially averaged velocity as a function of the PIV image number (ACT3 multi-DBD, 18kV, 1kHz)

Two different states are clearly noticeable: when the first plasma jet follows the wall curvature, the averaged velocity in the window is close to 2m/s and when the jet is separated the velocity is smaller than 0.5m/s. These two states are presented in the figures 9 and 10. The attached flow state represents 55% of the total 914 instantaneous fields and the unattached flow one contributes to 45%.

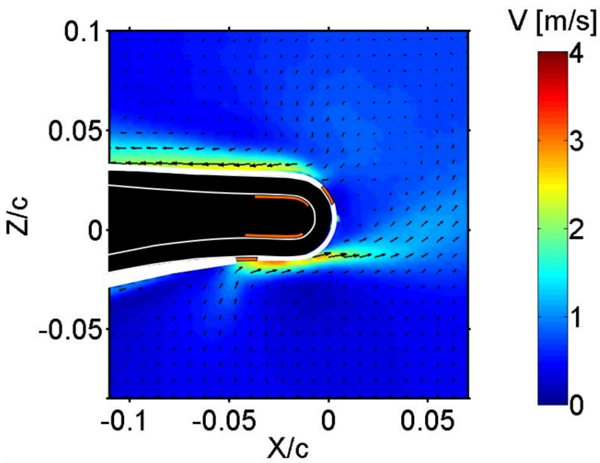

Figure 9 - Time averaged magnitude of the velocity contours and velocity vector field of the flow induced by the actuator 3 for the separated flow topology (ACT3, multi-DBD) (V=18kV, f=1kHz)

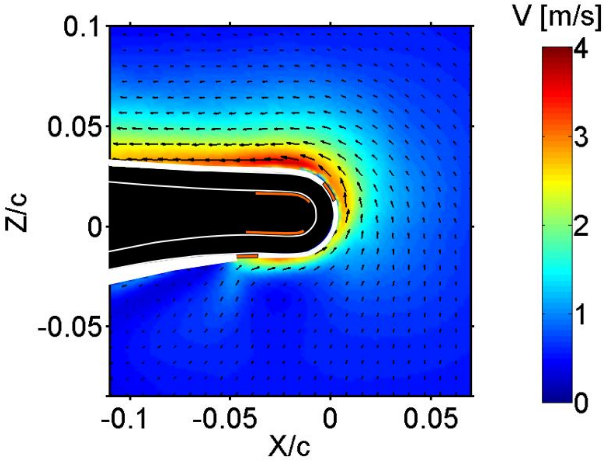

Figure 10 - Time averaged magnitude velocity contours and velocity vector field of the flow induced by the actuator 3 for the attached flow topology (ACT3, multi-DBD) (V=18kV, f=1kHz)

This phenomenon seems in relation with the voltage augmentation: the same actuator ACT3 powered at 15kV shows a time-averaged attached jet. Furthermore, the actuator ACT2 when powered at 20kV shows a fully unattached jet but an attached jet at 15kV and 18kV. Only the shifted configurations around the trailing-edge with an angle of 45º (ACT2 and ACT3) show for the higher voltage applications an unattached or intermittent unattached jet. Thus, the implementation of the floating electrodes aims to create an ionic wind cumulative effect between the actuators in order to ensure the jet attachment to the model wall.

C. *Influence of the floating electrodes*

All the actuators have been tested in a multi-DBD configuration as well as in an elongated-DBD one. The influence of the floating electrodes is presented for actuator ACT1. Figure 11 shows the difference of the velocity magnitude between the time averaged velocity fields corresponding to the flow induced by actuator 1 in multi-DBD configuration and the one corresponding to the elongated-DBD configuration. The floating electrodes seem to have a noticeable but small effect on the plasma jet topology. Indeed, the velocity of the ionic wind in the near wall is more important for the elongated-DBD configuration while the jet diffusion is greater for the multi-DBD case. However, the velocity difference is not greater than ±0.5m/s and the resulting wall jet modification is quite slight.

Regarding the unattached wall jet phenomenon, the floating electrodes permit the jet reattachment for the actuator ACT2 powered at 20kV. Concerning the actuator ACT3, the implementation of the floating electrodes suppresses the unsteadiness but the first DBD jet remains unattached to the wall.

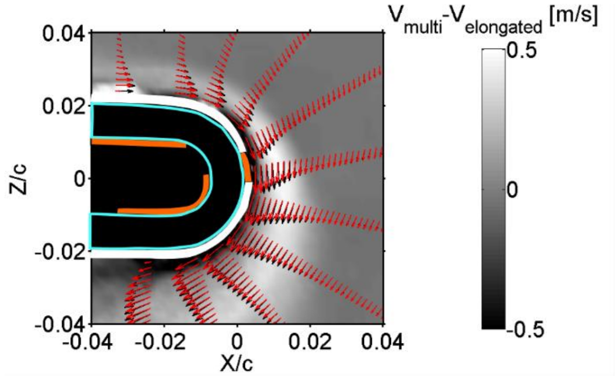

Figure 11 – Contours of velocity magnitude difference of the time averaged velocity field and velocity vector profiles of the flow induced by actuator 1 in multi-DBD (black vectors) configuration and elongated-DBD (red vectors) configuration (V=18kV, f=1kHz).

V. CONCLUSION

This paper presents the characterization of three sets of DBD actuators dedicated to implement a circulation control strategy in order to alleviate the lift force of a wind turbine blade. For such flow control strategy, it is necessary to understand and to deal with the induced flow attachment along a curved surface without relying on the Coanda effect. The jet topology induced by a DBD plasma actuator over a curved surface is then studied and it is shown that the flow induced by DBD does not always remain attached to the wall. At voltage amplitudes higher than 18kV, two configurations show a wall jet that doesn't follow the model surface. The influence of floating electrodes has also been analyzed: for the attached configurations they slightly change the flow topology at the near wall zone; for the unattached jet the elongated-DBD configuration may enable to maintain the jet attached to the curved surface. Further analysis and investigation are in progress to compare the wall jet evolution over such a curved surface in comparison with wall jet obtained along a plane surface or obtained with typical fluidic fence actuator as presented in [11].

ACKNOWLEDGMENTS

This project is funded by the French national project SMARTEOLE (ANR-14-CE05-0034).

REFERENCES

[1] R.D. Joslin, G. S. Jones, "Application of Circulation Control Technology," Volume 214. AIAA, Inc, 2006.
[2] J. Kweder, C.C. Panther, and J.E. Smith, "Applications of circulation control, yesterday and today," *Int. J. Eng.*, vol.4, pp.411–429, 2008.
[3] S.J. Johnson, C.P. Case van Dam and D.E. Berg, "Active Load Control Techniques for Wind Turbines," SANDIA Report, August 2008.
[4] N. Benard and E. Moreau, "Electrical and mechanical characteristics of surface AC

dielectric barrier discharge plasma actuators applied to airflow control", Experiments in Fluids, vol. 55, no. 11, 2014.
[5] M. Kotsonis, R. Pul and L. Veldhuis “Influence of circulation control on a rounded-trailing-edge airfoil using plasma actuators”, *Experiments in fluids*, 55(7), 2014.
[6] P. Zhang, B. Yan, a.B. Liu and J. J. Wang “Numerical simulation on plasma circulation control airfoil”, AIAA Journal, 48(10):2213-2226, 2010.
[7] A. Leroy, J. Podlinski, P. Devinant, and S. Aubrun, “Circulation control by plasma actuators for load fluctuation alleviation", 6th European Conference for Aeronautics and Space Science (EUCASS), 2015.
[8] A. Berendt, J. Podlinski, J. Mizeraczyk, “Elongated DBD with floating interelectrodes for actuators,” *Eur. Phys. J.-Applied Physics*, vol. 55, Issue: 1, 13804, 2011.
[9] M. Forte, J. Jolibois, J. Pons, E. Moreau, G. Touchard, M. Cazalens, “Optimization of a dielectric barrier discharge actuator by stationary and non-stationary measurements of the induced flow velocity: application to airflow control”. Experiments in Fluids 43:917–928, 2007.
[10] B. Dong, JM. Bauchire, JM Pouvesle, P. Magnier, D. Hong, “Experimental study of a DBD surface discharge for the active control of subsonic airflow”. J Phys D Appl Phys 41:155201, 2008.
[11] R. Neuendorf and I. Wygnanski, “On a turbulent wall jet flowing over a circular cylinder”, J. Fluid Mech., 381, 1-25, 1999.